Chinese Physics Letters

LETTER

Electronic Structure of a Correlated Antiferromagnetic Metal CrN in Epitaxial Thin Film Form

Cite as: Rui Xu *et al*. 2026 *Chin. Phys. Lett.* **43** 060711

DOI CSTR

Recommended Articles

Sr-Doping-Modulated Metal-Insulator Transition in $NdNiO_3$ Epitaxial Films

Huan Ye, Enda Hua, Fang Xu, Jingdi Lu, Feng Jin, Wenbin Wu, Liang Si, and Lingfei Wang
Chin. Phys. Lett. **41**, 117301 (2024)

The Effect of Carrier Doping and Thickness on the Electronic Structures of $La_3Ni_2O_7$ Thin Films

Haoliang Shi, Zihao Huo, Guanlin Li, Hao Ma, Tian Cui, Daoxin Yao, and Defang Duan
Chin. Phys. Lett. **42**, 080708 (2025)

From Ferromagnet to Antiferromagnet: Dimensional Crossover in (111) $SrRuO_3$ Ultrathin Films

Zhaoqing Ding *et al*.
Chin. Phys. Lett. **42**, 120709 (2025)

Effects of Thickness and Anisotropic Strain on Polarization Switching Properties of Sub-10nm Epitaxial $Hf_{0.5}Zr_{0.5}O_2$ Thin Films

Kuan Liu, Kai Liu, Xingchang Zhang, Jie Fang, Feng Jin, Wenbin Wu, Chao Ma, and Lingfei Wang
Chin. Phys. Lett. **41**, 117701 (2024)

Theory for Charge Density Wave and Orbital-Flux State in Antiferromagnetic Kagome Metal FeGe

Hai-Yang Ma, Jia-Xin Yin, M. Zahid Hasan, and Jianpeng Liu
Chin. Phys. Lett. **41**, (2024)

Centimeter-Scale Above-Room-Temperature Ferromagnetic Fe_3GaTe_2 Thin Films by Molecular Beam Epitaxy

Taikun Wang *et al*.
Chin. Phys. Lett. **41**, 107502 (2024)

A series journal of Chinese Physical Society distributed by IOP Publishing

iopscience.iop.org/cpl | cpl.iphy.ac.cn

Chinese Physics Letters

Chin. Phys. Lett. **43** 060711 (2026)

LETTER

DOI: 10.1088/0256-307X/43/6/060711
CSTR: 32039.14.0256-307X.43.6.060711

Electronic Structure of a Correlated Antiferromagnetic Metal CrN in Epitaxial Thin Film Form

Rui Xu(徐瑞)[1,2], Jiexiong Sun(孙捷雄)[1,2], Tongrui Li(李彤瑞)[1,2], Jianghao Yao(姚江浩)[1,2], Yuzhe Wang(王禹喆)[1,2], Xianglin Li(李祥霖)[1,2], Shiwu Su(苏世武)[1,2], Donglai Feng(封东来)[2,*], and Juan Jiang(姜娟)[1,2,*]

[1]Hefei National Research Center for Physical Sciences at Microscale and School of Emerging Technology, University of Science and Technology of China, Hefei 230026, China
[2]New Cornerstone Science Laboratory, Hefei National Laboratory, Hefei 230088, China

*Corresponding authors. Email: dlfeng@hfnl.cn; jjiangcindy@ustc.edu.cn

Chromium nitride (CrN) is a prototypical correlated antiferromagnet in which magnetic ordering is concomitant with a structural transition in its bulk form, yet its low-energy electronic structure in thin films remains largely unexplored. Here we investigate high-quality epitaxial CrN/MgO (001) thin films using angle-resolved photoemission spectroscopy (ARPES). Transport measurements reveal that the films remain metallic and undergo a magnetic transition without detectable structural distortion. ARPES directly resolves a shallow electron-like band crossing the Fermi level (E_F), forming a small Fermi surface that persists across the Néel temperature (T_N). A pronounced redistribution of spectral weight is observed, which may be related to the magnetic transition. Comparison with first-principles calculations shows that electronic correlations are essential to reproduce the observed band topology, establishing epitaxial CrN as a correlated antiferromagnetic (AFM) metal. These results help understand the interplay between magnetism, correlations, and lattice constraints in CrN, offering an example of tailoring electronic and magnetic properties in correlated AFM thin films.

Introduction

Transition-metal nitrides have garnered sustained interest due to their diverse electronic phases, strong electron correlations, and compatibility with epitaxial thin-film growth. These characteristics provide a fertile ground for both fundamental studies and functional applications [1−8]. Among these materials, CrN occupies a unique position as a correlated antiferromagnet whose electronic, magnetic, and structural degrees of freedom are intricately intertwined.

In bulk CrN, AFM ordering emerges below $T_N \sim 280$ K. At the same temperature, the lattice undergoes a structural transition from the cubic NaCl-type phase ($Fm\bar{3}m$) to an orthorhombic phase ($Pnma$), while the transport behavior evolves from insulating (or semiconducting) to metallic [9−12]. Such coupled transitions have attracted broad research interest regarding their mechanisms and tuning. Theoretical calculations indicate that CrN exhibits marginal Mott behavior, with its low-energy electronic states highly sensitive to correlation strength, magnetic disorder, and lattice distortions [13−17]. The structural transition is primarily associated with lattice distortions driven by the onset of magnetic ordering [9,18,19]. The metal-insulator transition is thought to result from a combination of correlation effects, changes in magnetic disorder-induced scattering, and the concomitant structural distortion [12,17,20]. Taken together, the evolution of structural, magnetic, and transport properties is understood to arise from the interplay between multiple degrees of freedom, reflecting a delicate balance among competing phases.

Epitaxial thin films serve as a versatile platform for tailoring electronic and physical functionalities. Recent transport studies have revealed that in thin films, the bulk-like structural transition and metal-insulator transition are notably suppressed, leading to persistent metallic behavior across the magnetic transition [21−25]. This deviation strongly suggests that the magnetic, structural, and metal-insulator transitions can be decoupled through interface effects. Such decoupling provides an opportunity to identify the dominant factors underlying these intriguing properties. Despite these advances, the microscopic origin of the thin-film behavior remains elusive. Systematic momentum-resolved measurements of the electronic structure across the AFM transition are therefore essential for understanding the underlying physics of this system.

In this work, we investigate epitaxial CrN thin films using low-energy electron diffraction (LEED), transport, and ARPES. Transport and temperature-dependent LEED measurements reveal an AFM transition with the system remaining metallic across the transition and without detectable structural symmetry change, in contrast to bulk CrN. High-resolution ARPES results directly resolve a shallow electron-like band crossing E_F, confirming metallic behavior. Across the AFM transition, there is a pronounced redistribution of spectral weight over a broad energy range, which provides spectral evidence of the magnetic transition. Comparison with first-principles calculations indicates that including electronic correlations is essential to reproduce the observed band structure. Together, these results establish the epitaxial CrN/MgO (001) thin films as a correlated AFM metal, where the magnetic transition occurs independently of the structural and metal-insulator transitions observed in bulk CrN, reflecting the significant influence of epitaxial strain and interfacial effects on the correlated electronic structure.

Results

Epitaxial Growth and Structural Characterization. High-quality epitaxial CrN thin films with a thickness of ~12.5 nm were grown on single-crystal MgO (001) substrates by nitrogen-assisted reactive molecular beam epitaxy (MBE) [see Section S1 in the Supplementary Material (SM)]. The crystalline quality and phase purity of the films were evaluated by different characterization methods. As shown in Fig. 1(a) from the X-ray diffraction (XRD) result, the CrN (002) film peak exhibits clear Laue oscillations alongside the MgO (002) substrate peak. No additional diffraction peaks associated with secondary phases or impurities were observed within the instrumental resolution in the XRD pattern measured over a wider 2θ range (see Fig. S1 in the SM), confirming single-phase growth and high crystalline quality of the thin film. Reciprocal space mapping (RSM) around the asymmetric (113) reflection shown in Fig. 1(b) reveals that the in-plane

Received 24 March 2026; accepted 28 April 2026; published 16 June 2026
© 2026 Chinese Physical Society and IOP Publishing Ltd. All rights, including for text and data mining, AI training, and similar technologies, are reserved.

Check for updates

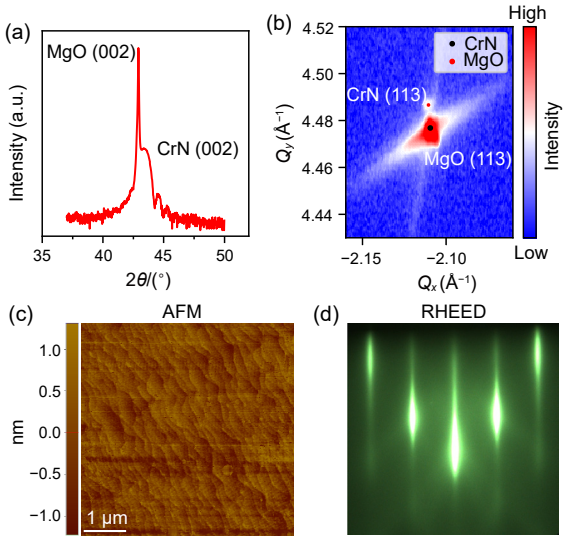

Fig. 1. Structural characterization of epitaxial CrN (001) thin films grown on MgO (001). (a) θ–2θ scan of CrN/MgO (001) thin film from XRD. (b) RSM result around the asymmetric CrN (113) reflection. (c) Atomic force microscopy image of as-grown CrN thin film, showing step terraces. (d) RHEED pattern of the as-grown thin film.

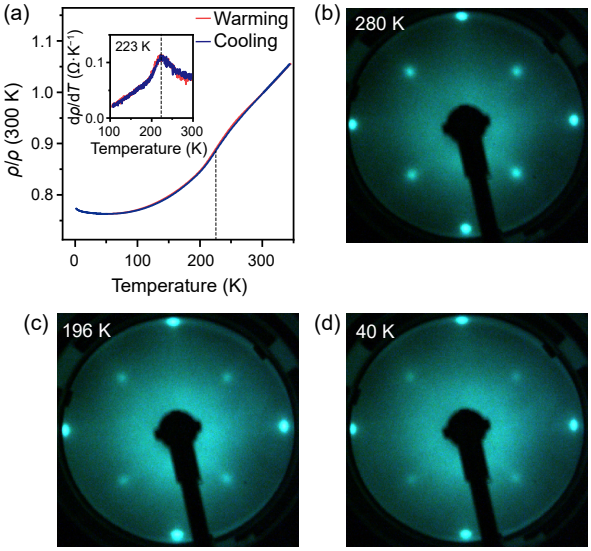

Fig. 2. Temperature-dependent transport and LEED results. (a) Temperature dependence of the normalized resistivity $\rho(T)/\rho(300\ \mathrm{K})$ measured from 2 K to 300 K, showing metallic behavior over the entire temperature range. The inset displays the first derivative $\mathrm{d}\rho/\mathrm{d}T$, highlighting a broad anomaly around $T_N \sim 223$ K associated with the AFM transition. (b)–(d) LEED patterns acquired at 280 K, 196 K, and 40 K, respectively.

reciprocal lattice position of the CrN peak closely coincides with that of the MgO substrate. This indicates that the CrN films are coherently strained by the MgO substrate along the in-plane directions, corresponding to an in-plane tensile strain of approximately 1.7%.

The surface morphology of the CrN films was characterized by both atomic force microscopy and reflection high-energy electron diffraction (RHEED). The 5 μm × 5 μm atomic force microscopy image shown in Fig. 1(c) reveals atomically flat terraces separated by well-defined step edges, with a root-mean-square roughness of ~0.5 nm. The RHEED pattern in Fig. 1(d) exhibits sharp streaks, indicating a smooth and well-ordered crystalline surface. We note that nitrogen-related defects can influence transport and magnetism in CrN [13,15,26]. Within our growth window, systematic variations of the nitrogen partial pressure over a moderate range did not produce discernible changes in crystal quality, the temperature of the transport anomaly, or the Fermi-surface topology (see Section S3 and Figs. S2 and S3 in the SM). Therefore, all the thin films obtained are representative of the nitrogen-sufficient growth condition.

Transport Anomaly and Temperature-Dependent LEED. Figure 2(a) presents the temperature dependence of the normalized resistivity $\rho(T)/\rho(300\ \mathrm{K})$ of the CrN thin film. The resistivity shows an overall decrease upon cooling, indicating metallic behavior over the entire measured temperature range up to 300 K. An anomaly appears near 223 K, which is more pronounced in the first derivative of the resistivity ($\mathrm{d}\rho/\mathrm{d}T$) as a broad peak, consistent with the AFM transition of CrN thin films reported previously [21,24,25]. Such a transition temperature is significantly lower than that reported for bulk CrN, which can be primarily attributed to the combined effects of epitaxial-strain induced changes in the magnetic exchange interactions [17,18,20] and reduced dimensionality [27,28]. Within our experimental resolution, no discernible thermal hysteresis is detected between the heating and cooling cycles. This contrasts with bulk CrN, where the AFM transition occurs simultaneously with a structural transition and exhibits a pronounced first-order-like hysteresis. In epitaxial thin films, however, the structural transition is strongly suppressed by epitaxial strain, and the transition becomes predominantly magnetic in nature, which is expected to be closer to a continuous transition and thus does not exhibit noticeable hysteresis. The absence of hysteresis in our epitaxial films suggests that the structural transition is suppressed, and the magnetic transition occurs independently of lattice symmetry changes [10,12].

To probe the near-surface structural response across this transition under the same *in situ* conditions as the ARPES measurements, temperature-dependent LEED measurements were carried out. As shown in Figs. 2(b)–2(d), the (1×1) diffraction patterns observed at 280 K ($T > T_N$) remain sharp and well-defined down to 40 K ($T < T_N$), without any detectable spot splitting or additional superstructure within our experimental sensitivity, providing an important reference for the absence of the structural transition in the CrN thin films. This observation is also consistent with previous temperature-dependent XRD and RHEED studies on epitaxial CrN thin films, where the structural transition is strongly suppressed under epitaxial strain [22,23].

Taken together, the resistivity and LEED results indicate that, in our epitaxial CrN thin films, the observed transition is primarily magnetic in nature. Within the experimental resolution, we find no evidence for a structural transition or a metal–insulator transition, suggesting that the magnetic ordering occurs independently of lattice symmetry changes or large-scale electronic localization.

Correlated Metallic Electronic Structure in CrN Thin Films Revealed by ARPES. To investigate the electronic structure of CrN thin film, we performed ARPES measurements at 10 K, with an overall energy resolution of approximately 10 meV under this configuration. Figure 3(a) presents the momentum-integrated EDCs derived from ARPES intensity over a broad energy range, spanning from E_F down to 10 eV binding energy. Multiple prominent peaks are observed, forming a broad valence band structure which is typical of transition-metal nitrides. For comparison, figure 3(b) shows the calculated density of states (DOS) for cubic AFM CrN obtained from DFT+U calculations with $U = 3.0$ eV and $J = 0.94$ eV where the interaction parameters are adopted from previous reports [14,16,29]. The calculated DOS reproduces the main features of the experimental valence band over a wide energy range, indicating a reasonable description of the occupied electronic states. The differences in spectral weight distribution may arise from matrix-element effects associated with the photon energy (He I α, ~21.2 eV) used in our measurements. Comparing the experimental and calculation results, the band features observed from E_F to −3 eV are primarily composed of Cr-derived orbitals, while those from −3 eV to −8 eV arise from Cr–N hybrid states. The finite intensity at E_F indicates a gapless metallic state in the CrN thin film.

Figure 3(c) shows the Fermi surface of the CrN film, where a Fermi pocket with finite spectral weight is observed. The dispersion cut

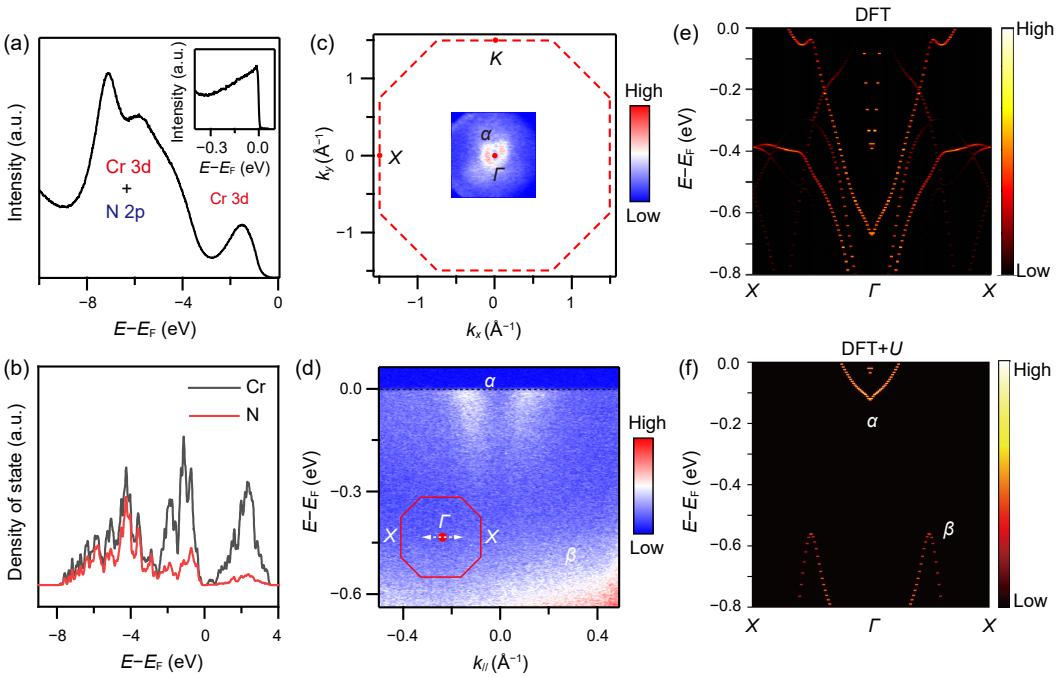

Fig. 3. Electronic structure of CrN thin films measured by ARPES. (a) EDC from E_F to 10 eV binding energy obtained by integrating the ARPES intensity over a k-range of ±0.5 Å^{-1}; inset: enlarged spectra near E_F. (b) Calculated DOS using DFT+U with $U = 3.0$ eV and $J = 0.94$ eV for the cubic AFM CrN. (c) Fermi surface mapping obtained by integrating the ARPES intensity within ±10 meV around E_F. (d) High-resolution ARPES cut along Γ–X near E_F, showing a shallow electron-like α band crossing E_F; inset: corresponding momentum location of the cut in the Brillouin zone. (e) and (f) Calculated band structure along corresponding high-symmetry direction using DFT and DFT+U methods, respectively. All ARPES data were collected at 10 K.

along the Γ–X direction near E_F [Fig. 3(d)] reveals a shallow electron-like band and the signature of another deeper-lying band, which we refer to as the α and β bands, respectively (see Fig. S4 in the SM for detailed analysis of the β band). In contrast, the corresponding DFT-calculated band structure [Fig. 3(e)], as well as the DFT+U calculation for the non-magnetic (NM) state (see Fig. S5 in the SM) exhibit substantial discrepancies in low-energy band topology. Only the DFT+U calculation for the AFM state ($U = 3$ eV, $J = 0.94$ eV) [Fig. 3(f)] qualitatively captures the overall band structure, after an energy shift of ~ 0.3 eV, supporting that correlation effects and AFM order are essential for accurately describing the low-temperature electronic structure in CrN/MgO (001) thin films.

Notably, the α band extends to approximately 0.3 eV below E_F, indicating a relatively shallow electronic structure near E_F. k_z-dependent DFT+U calculations further reveal that the band crossing E_F appears only in the vicinity of $k_z = 0$, implying that the corresponding Fermi surface occupies a very small volume in the three-dimensional Brillouin zone (see Fig. S6 in the SM). Such a shallow Fermi crossing and tiny Fermi-surface volume suggest that the system may lie in the vicinity of a metal–insulator transition. In this critical regime, external perturbations such as strain, doping, or defect engineering can readily drive the system into insulating or semiconducting states. Combined with the transport measurements, these results suggest that the epitaxial CrN/MgO (001) thin films are a correlated AFM metal, and may lie on the verge of a metal-insulator transition.

Persistent Metallic Electronic Structure and Spectral Weight Redistribution Across the AFM Transition. To probe the electronic response across the AFM transition, we performed temperature-dependent ARPES measurements. Figures 4(a) and 4(b) show the ARPES intensity maps at the E_F measured above ($T > T_N$) and below ($T < T_N$) the AFM transition, respectively. Within the experimental resolution, the overall Fermi surface topology remains nearly unchanged across the transition. The most notable modification from 40 K to 270 K is the reduction of coherent spectral weight and an apparent broadening of the linewidth near E_F. The band dispersion of the α band along the Γ–X direction crossing E_F at $T > T_N$ and $T < T_N$ are shown in Figs. 4(c) and 4(d), respectively. There is no observable gap opening within our detectable range. The band positions and dispersion slopes are largely preserved, indicating that the system remains metallic on both sides of the transition.

While the low-energy band topology remains unchanged, pronounced changes are observed in the spectral weight distribution. Figure 4(e) compares EDCs collected from high-T and low-T phases. The main peak positions show no significant shifts, suggesting that any possible aging-induced chemical-potential drift is minimal compared to the overall spectral changes. Upon warming into the paramagnetic (PM) phase, the spectral weight near E_F is reduced, while spectral weight at deeper binding energies increases. This behavior is reversible upon cooling back into the AFM state, indicating that it is intrinsic. Meanwhile, the increase in spectral weight at higher binding energies indicates that the change is not due to a uniform suppression of the entire spectrum, but rather reflects a redistribution of spectral weight. Given the absence of a structural transition in our thin films, the observed behavior is most likely governed by the AFM transition and the associated magnetic disorder, which strongly modifies the electronic states via enhanced scattering effects. Similar trends have been observed in correlated AFM metals such as α-$Fe_{1.06}Te$ [30,31], and a similar mechanism may apply to our epitaxial CrN thin films.

Discussion

Figure 4(f) summarizes the central physics picture we propose based on our observations. In the PM state, strong spin-fluctuation and magnetic disorder likely increase the scattering rate of Cr 3d electrons, thereby suppressing low-energy electronic coherence near E_F, resulting in a reduced spectral weight at E_F dominated by Cr 3d states, as well as a broadening of spectral features. Upon cooling below T_N into the AFM state, the formation of AFM order may suppress spin-disorder scattering. As a result, the spectral weight near E_F becomes partially recovered and more coherent, and this redistribution is reflected experimentally as an increase in spectral weight of Cr 3d states at low binding energies over a broad energy range. This

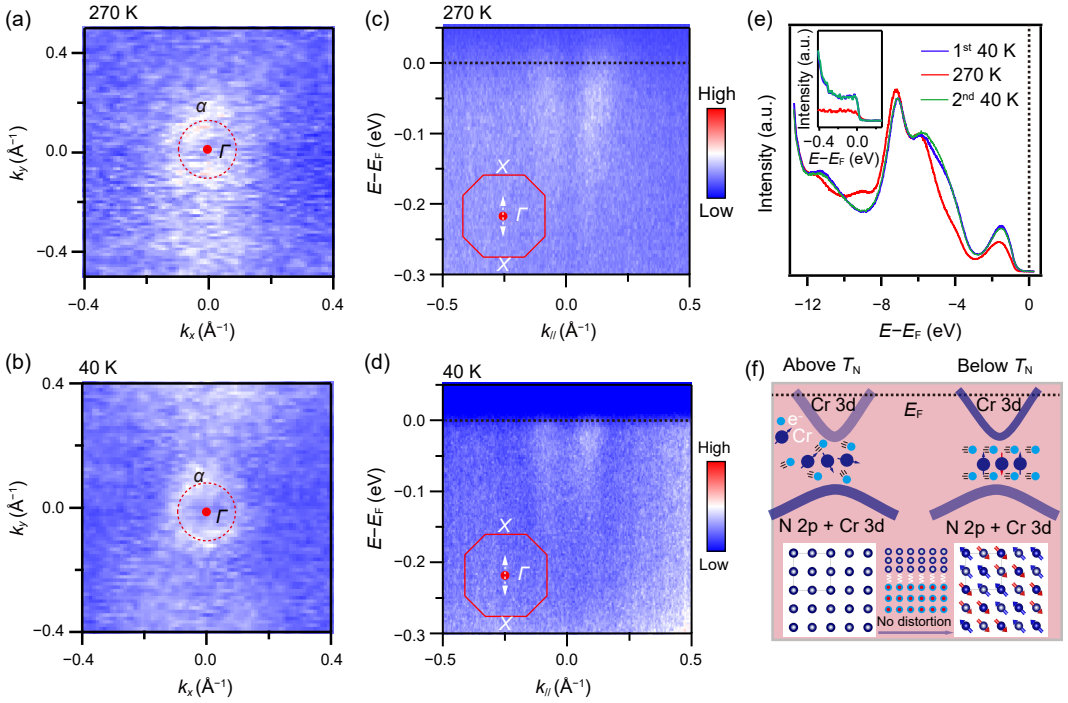

Fig. 4. Temperature-dependent ARPES measurements of CrN thin films across the AFM transition. (a) and (b) Fermi surface intensity maps measured at high temperature ($T > T_N$) and low temperature ($T < T_N$), respectively. (c) and (d) Representative ARPES dispersion cuts taken along Γ–X at 270 K and 40 K, respectively; inset: corresponding momentum locations of the cuts in the Brillouin zone. (e) Energy distribution curves (EDCs) integrated over a k range of ±0.5 Å^{-1}, spanning binding energies from E_F to 12.5 eV. Inset: an enlarged view of the EDCs near E_F. (f) Schematic illustration summarizing the central physical scenario in CrN thin film.

picture is consistent with previous reports showing that magnetic disorder in CrN strongly influences its electronic structure and transport properties [12,20]. Meanwhile, because the lattice is pinned by epitaxial strain, any structural transition is strongly suppressed.

Regarding the absence of the metal-insulator transition, from the perspective of electronic structure, CrN in the thin-film form exhibits marginal metallic behavior that is highly sensitive to external tuning parameters. In bulk CrN, the structural transition may act as a driving force for the metal-insulator crossover; however, in the strain-locked thin-film system, this structural transition is greatly weakened, which may lead to the suppression of such a metal-insulator transition. Overall, the epitaxial strain pins the lattice, suppressing structural change and may effectively eliminate the metal-insulator transition. This decoupling of the magnetic transition from structural and metal–insulator transitions highlights the unique role of epitaxial strain in selectively tuning correlated electronic states.

Conclusions

In summary, we systematically investigate the electronic structure as well as the structural and transport behavior of epitaxial CrN/MgO (001) thin films. Comparisons of ARPES results and DFT+U calculations establish a correlated AFM metallic electronic structure that persists across T_N, with a pronounced redistribution of spectral weight over a broad energy window, reflecting the influence of AFM ordering. The small Fermi volume of this metallic band further suggests that the system lies near a metal–insulator crossover and may be sensitive to external tuning. The suppression of structural transition under epitaxial strain likely contributes to the absence of an insulating transition. These findings provide a momentum-resolved reference for the correlated AFM metallic nature of CrN/MgO (001) thin films and highlight how epitaxial strain can selectively decouple magnetic, structural, and electronic degrees of freedom, offering a model platform to explore and control correlation-driven phenomena in transition-metal nitride thin films.

Acknowledgements

This work was supported by the National Key R&D Program of China (Grant No. 2023YFA1406304), the National Natural Science Foundation of China (Grant No. 12574071), the Quantum Science and Technology-National Science and Technology Major Project (No. 2021ZD0302803), and the New Cornerstone Science Foundation.

References

[1] Papaconstantopoulos D A, Pickett W E, Klein B M, and Boyer L L 1985 *Phys. Rev. B* **31** 752
[2] Lévy F, Hones P, Schmid P, Sanjinés R, Diserens M, and Wiemer C 1999 *Surf. Coat. Technol.* **120-121** 284
[3] Chockalingam S P, Chand M, Jesudasan J, Tripathi V, and Raychaudhuri P 2008 *Phys. Rev. B* **77** 214503
[4] Ningthoujam R and Gajbhiye N 2015 *Prog. Mater. Sci.* **70** 50
[5] Yu T, Wright J, Khalsa G *et al.* 2021 *Sci. Adv.* **7** eabi5833
[6] Wang H, Li J, Li K, Lin Y, Chen J, Gao L, Nicolosi V, Xiao X, and Lee J M 2021 *Chem. Soc. Rev.* **50** 1354
[7] Cheng Z, Qi W, Pang C H, Thomas T, Wu T, Liu S, and Yang M 2021 *Adv. Funct. Mater.* **31** 2100553
[8] Yao J, Li T, Zhi A *et al.* 2025 *Adv. Funct. Mater.* **35** 2417638
[9] Corliss L M, Elliott N, and Hastings J M 1930 *Phys. Rev.* **117** 929
[10] Browne J D, Liddell P R, Street R, and Mills T 1970 *Phys. Status Solidi A* **1** 715
[11] Mrozińska A, Przystawa J, and Sòlyom J 1979 *Phys. Rev. B* **19** 331
[12] Bhobe P A, Chainani A, Taguchi M *et al.* 2010 *Phys. Rev. Lett.* **104** 236404
[13] Gall D, Shin C S, Haasch R T, Petrov I, and Greene J E 2002 *J. Appl. Phys.* **91** 5882
[14] Herwadkar A and Lambrecht W R L 2009 *Phys. Rev. B* **79** 35125
[15] Rojas T and Ulloa S E 2008 *Phys. Rev. B* **98** 214111
[16] Cheiwchanchamnangij T and Lambrecht W R L 2020 *Phys. Rev. B* **101** 85103
[17] Biswas B, Rudra S, Rawat R S *et al.* 2023 *Phys. Rev. Lett.* **131** 126302
[18] Filippetti A, Pickett W E, and Klein B M 1999 *Phys. Rev. B* **59** 7043
[19] Filippetti A and Hill N A 2000 *Phys. Rev. Lett.* **85** 5166

[20] Alling B, Marten T, and Abrikosov I A 2010 *Phys. Rev. B* **82** 184430
[21] Inumaru K, Koyama K, Imo-oka N, and Yamanaka S 2007 *Phys. Rev. B* **75** 54416
[22] Zhang X Y, Chawla J S, Deng R P, and Gall D 2011 *Phys. Rev. B* **84** 73101
[23] Alam K, Disseler S M, Ratcliff W D *et al*. 2017 *Phys. Rev. B* **96** 104433
[24] Jin Q, Wang Z, Zhang Q *et al*. 2021 *Phys. Rev. Mater.* **5** 23604
[25] Jin v, Cheng H, Wang Z *et al*. 2021 *Adv. Mater.* **33** 2005920
[26] Gall D, Shin C S, Spila T, Odén M, Senna M J H, Greene J E, and Petrov I 2002 *J. Appl. Phys.* **91** 3589
[27] Brookes N, Chang Y, and Johnson P 1991 *Phys. Rev. Lett.* **67** 354
[28] Weschke E, Ott H, Schierle E *et al*. 2004 *Phys. Rev. Lett.* **93** 157204
[29] Kalal S, Nayak S, Sahoo S, Joshi R, Choudhary R J, Rawat R, and Gupta M 2023 *Sci. Rep.* **13** 15994
[30] Zhang Y, Chen F, He C *et al*. 2010 *Phys. Rev. B* **82** 165113
[31] Dai Y M, Akrap A, Schneeloch J, Zhong R D, Liu T S, Gu G D, Li Q, and Homes C C 2014 *Phys. Rev. B* **90** 121114